Water Science & Technology

IWA PUBLISHING

Water Science & Technology Vol 85 No 6, 1855 doi: 10.2166/wst.2022.079

Ayurvedic hospital wastewater degradation using electrochemical treatment

S. Mahesh [a,*], K. S. Shivaprasad [b] and Mahesh Sanjana [c]

[a] Department of Environmental Engineering, Sri Jayachamarajendra College of Engineering, Constituent College of JSS Science and Technology University (Formerly SJCE), JSSTI Campus, Mysuru, Karnataka State 570006, India
[b] Department of Environmental Engineering, Sri Jayachamarajendra College of Engineering, Constituent College of JSS Science and Technology University, JSSTI Campus, Mysuru, Karnataka State 570006, India
[c] JSS Ayurveda Medical College, Lalitadripura Road, Alanahalli, Mysuru, Karnataka State 570028, India
*Corresponding author. E-mail: maheshs@sjce.ac.in

SM, 0000-0002-7002-8514; KSS, 0000-0002-3322-6554; MS, 0000-0002-3619-4826

ABSTRACT

The goal of this research was to remove COD, oil and grease (O&G) and color from raw ayurvedic hospital wastewater (AHWW) using a novel electrochemical coagulation (ECC) process. Cell voltage was initially optimized using iron electrodes in bipolar mode for both raw AHWW and ayurvedic hospital therapy room wastewater (AH-TRWW) for a pre-optimized electrolysis time (ET) of 60 min. O&G, COD and color removals for AHWW at 8 V optimized cell voltage were 96, 61 and 96% respectively. Different electrode materials, copper, aluminum, graphite, were used to evaluate relative performances at 8 V. Iron electrodes showed maximum pollutant removal from raw AHWW. The sludge obtained after the ECC process showed good settling and filterability properties compared to graphite and aluminum electrodes. The low SVI value of 146 mL/g was obtained exercising absolute control on sludge volume. Solids flux values showed assurances of compact settling tank design with least spatial footprint. EDX analysis for ECC sludge of AHWW using iron showed gross elements 40.19% C, 48.63% O and 7.92% Fe redefining the fate of sludge. The XRD pattern of the ECC sludge showed an amorphous nature. Post-ECC filtration effluent showed clear water reclamation of 80–82%, proving the effectiveness of the novel ECC treatment process.

Key words: COD, ECC, electrode, oil and grease, sludge-EDX, water reclamation

HIGHLIGHTS

- Electrochemical coagulation of real ayurvedic hospital wastewater.
- Lowest HRT is achieved for maximum pollutant/contaminants removal.
- Water reclamation is possible using an ECC process.
- ECC reduces spatial and energy footprint

GRAPHICAL ABSTRACT

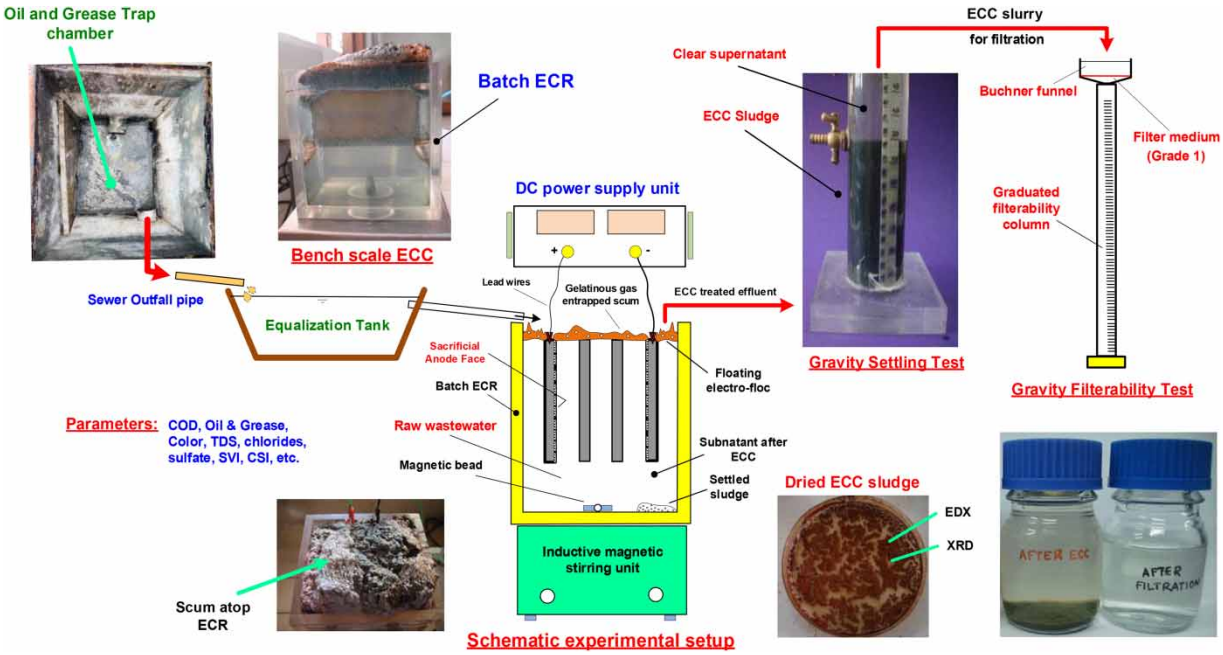

INTRODUCTION

In developing countries, less attention is paid to wastewaters generated from hospitals, medical research laboratories, health care institutions and pathology laboratories for reasons ascribed to direct disposal of pathogenic/toxic substances and non-metabolized pharmaceuticals into the sewers and the aquatic environment. Ayurveda, an ancient vedic medicinal science, is based on five major elements governing three basic factors, Pitta (P), Kapha (K) and Vata (V). An imbalance in these three different factors causes several diseases and disorders. Numerous ayurvedic treatment remedies intend to relax the patient, relieve stress, reduce emotional blockages and reinstate balance between PKV in humans. Herbal formulations in ayurvedic medicines are fast-growing industries spread all over the globe. Though ayurvedic formulations are mostly based on herbs, synthetic materials are also added during manufacturing, and while rendering patient services. The intent of these formulations is to bring back the lost balance in the PKV. The various chemicals added during drug formulations include glucose, jaggery, alcohol, gelatin, lactose, clay, mineral salts and several other organic solvents. These industries generate wastewaters having a high strength containing alkaloids, extracts from plants and trace minerals.

Most hospitals in urban areas discharge their liquid waste stream into the existing sewerage system without any pre-treatment and therefore the biodegradability of the domestic wastewaters reduces on reaching the treatment facility. In hospitals, a large variety of substances and chemical formulations are used for different medical purposes, diagnostics and research. After their use, >90% of these substances reach the waste stream using water as a medium. Liquid wastes generated by health care activities include a broad range of chemicals, disinfectants, small swabs, amputated tissue, diagnostic samples, blood, body fluids, surfactants, pharmaceuticals etc. Therapy room wastewaters are contaminated with oil and grease (O&G), particulate solids, biochemical oxygen demand (BOD_5), chemical oxygen demand (COD) and suspended solids (SS), which may cause serious pollution and contamination of water courses near by the hospitals. A clear legal protocol is yet to be framed for effective treatment of oily contaminated wastewater generating from these ayurvedic hospitals. These wastewaters differ significantly and vary in flow characteristics from allopathic healthcare facility wastewaters. In ayurvedic hospitals, the liquid waste generated from certain therapies such as Vamana, Virechana, Raktamoksha, Basti etc. are disposed using traditional treatment processes. The priority pollutants in ayurvedic hospital wastewaters are COD, fat, color, O&G, BOD, dissolved solids, trace chemicals and metals. The kashayas (decoction) and liquids other than taila (oils) used for Dhara, Avagaha (similar to tub bath), Salvana, Upanaha, Ksalana are also disposed into the natural drains. Most of these herbal preparations do not cause any issues until and unless they are properly drained into the sewerage system. Otherwise stagnant

liquid wastes emit foul odor and promote breeding of flies (Rajan *et al.* 2019). The very scant research on treating raw ayurvedic wastewater prompted us to take up this novel research work.

In this work, we investigate the use of an electrochemical coagulation (ECC) process for treating real ayurvedic hospital wastewater (AHWW) and ayurvedic hospital therapy room wastewater (AH-TRWW) stream for removing the aforesaid prime pollutants. Raw AHWW and TRWW were collected and characterized as per APHA procedures for important quality parameters before commencing batch ECC using two dimensional metal plate electrodes made of different metals. The importance of using advanced treatment of tough wastewaters is to grossly reduce the hydraulic retention time (HRT) and to reduce the total number of unit operations and processes in the treatment train, and achieve a state of mineralization.

ECC has been successfully used for removal of a variety pollutants from different wastewaters such as electroplating wastewater (Adhoum *et al.* 2004), slaughterhouse wastewater (Kobya *et al.* 2006), dairy wastewater (Sengil & Ozacar 2006), automobile garage wastewater (Harinarayanan *et al.* 2016), laundry wastewater (Dimoglo *et al.* 2019), sunflower oil refinery wastewater (Sharma *et al.* 2020) and chocolate industry wastewater (Garcia-Orozco *et al.* 2021). The challenges faced in our earlier research were – to achieve the lowest-possible HRT and good floc settleability, and to obtain clear water after ECC with gravity filtration, sludge volume index (SVI) control and sturdy ECC sludge. These challenges were successfully overcome in the current research treating raw AHWW.

Impacts of biomedical service industry wastewaters on environmental attributes

Biomedical industry wastewaters include wastewaters generating from hospitals governing allopathic, ayurvedic and homeopathic treatment facilities and pathology laboratories. Allopathic and ayurvedic hospitals treating patients generate tough and recalcitrant liquid waste streams constituting a combination of drugs, pathogens, organic chemicals, disinfectants, blood products and body fluids, buffers, dilute mineral acids/bases, high phosphate concentrations, oxidizers, oil and particulate materials. AHWW consists of a very complex water matrix loaded with pathogens, trace metals, high levels of O&G, total suspended and dissolved solids. Direct discharge of pollutant-loaded effluents into the urban sewerage systems without treatment can cause potential hazard to the environment. The critical parameters concerning ayurvedic hospital wastewaters are COD, and O&G color and TDS. O&G in the raw wastewater stick to the internal surfaces of the sewer lines reducing the effective flow area and subsequently block the flow (Wallace *et al.* 2016). It may also cause flooding and sewer overflows, especially in combined systems (Keener *et al.* 2008) resulting in growth of bio-slimes causing corrosion of piping and equipment (He *et al.* 2013).

Toxic disinfecting chemicals used in hospitals are loaded with sulfate and phosphate, and when discharged without adequate treatment into the aquatic environment destroys aquatic life (Kumari *et al.* 2020) resulting in dead lakes. Hospitals also discharge toxic pollutants such as mercury, silver, cyanide, formaldehyde etc. (Emmanuel *et al.* 2004; Yasar *et al.* 2013). These pollutants pose serious threat to soil and water attributes ultimately reaching the human food chain through any of the three routes – oral ingestion, inhalation and dermal contact. One of the major issues associated with ayurvedic hospitals and therapy centers is water mixed with oil and mudga churna (barley powder), which generates wastewater after a shower is taken by patients undergoing abyanga (oil massage), udwartana (powder massage) or other therapeutic procedures. The oil-laden waste stream can clog piping infrastructure resulting in malodor and corrosion. This wastewater on reaching the natural drains adversely affects the useful bacterial flora. The presence of fat, oil and grease (FOG) frequently causes problems for both on-site sewage disposal systems and off-site public sewerage systems (Abd El-Gawad 2014). The problem is aggravated when O&G liquefy at high water temperatures during housekeeping practices and later solidify within the sewer lines and on sensitive soil interfaces in leaching facilities of on-site treatment systems. High grease loads, emulsified grease and surge wastewater loadings often cause grease to bypass grease traps and enter the treatment system. The FOG on reaching the soil absorption system physically clog the soil pores preventing infiltration and also decrease in the oxygen content in soil. High BOD_5 present in FOG accelerates excessive bacterial growth and cause formation of a thick anaerobic biomass leading to premature failure of the soil absorption system.

Ayurvedic hospital – sources and wastewater flow

The ayurvedic hospital chosen in this research work is equipped with over 150 beds and specialty wards. The outpatient department (OPD) caters to several treatment options as per the needs of the patients. The lead hospital is also equipped with operating theaters and emergency wards to meet emergency and critical cases. The hospital offers treatment for several disorders and diseases such as arthritis, lumbago (low back ache), sciatica, spondylitis, paralysis, ENT, obesity, asthma,

allergy, fistula, skin disorders, rheumatoid arthritis, musculo-skeletal dysfunction, piles, menstrual disorders etc. Most ayurvedic hospitals rely on their own groundwater sources to meet their daily water requirements. After the water is used in several therapies, the wastewater generated is loaded with toxicants, FOG, COD, BOD_5, solids and trace metals. On an average, the total wastewater generation (including in-house canteen) ranges from 300 to 600 liters per bed per day (Lpbpd). Commonly, the effluent treatment in most ayurvedic hospitals includes a small FOG trap (Figure 1(a)), media filtration, chlorine disinfection and temporary storage for secondary use later.

So far, no work is reported on the treatment of specialized wastewaters like wastewaters from ayurvedic formulation units. Only one work is reported (Singh *et al.* 2016) on ECC of ayurvedic pharmaceutical (formation unit) wastewater focusing on COD and color removal using response surface methodology. Because of the toxic nature of raw ayurvedic wastewater with O&G content, the biological treatment fails because of microbe masking by oil content in the wastewater, and consequently ECC is proposed in our research work. The ayurvedic wastewater chosen in this research work is from a leading ayurvedic hospital treating inpatients and outpatients. This research shows a focus on using ECC for removal of pollutants from raw ayurvedic hospital wastewater and to reach a state of mineralization.

The ECC process offers the lowest treatment times (hydraulic retention times; HRT) compared to other traditional/advanced wastewater treatment processes (Mahesh *et al.* 2016) offering a small spatial footprint. Further, the total number of unit operations and unit processes can be greatly reduced. An added advantage is that the SVI can be easily controlled by the cell voltage applied in an ECC treatment system.

MATERIALS AND METHODS

Raw wastewater collection

Raw AHWW and AH-TRWW samples were collected as and when required from the outfall pipe with necessary precautions using grab sampling technique on high and low mass load days. The samples were brought to the laboratory and preserved at 4 °C before parameter analyses. Characterization and ECC experiments were carried out on real wastewater after normalizing it to ambient room temperature.

Parameter analyses

Quality parameters pH, temperature, conductivity and color were measured on-site at the time of raw wastewater sampling. The remaining parameters were analyzed in the laboratory. Procedures described in APHA Standard Methods 2017 were used for analyzing various parameters and recorded as C_o (initial parameter value) for the chosen parameters. Solids were determined using gravimetry, whereas BOD_5, COD, total alkalinity as $CaCO_3$, total hardness, chloride, phosphate and sulfate

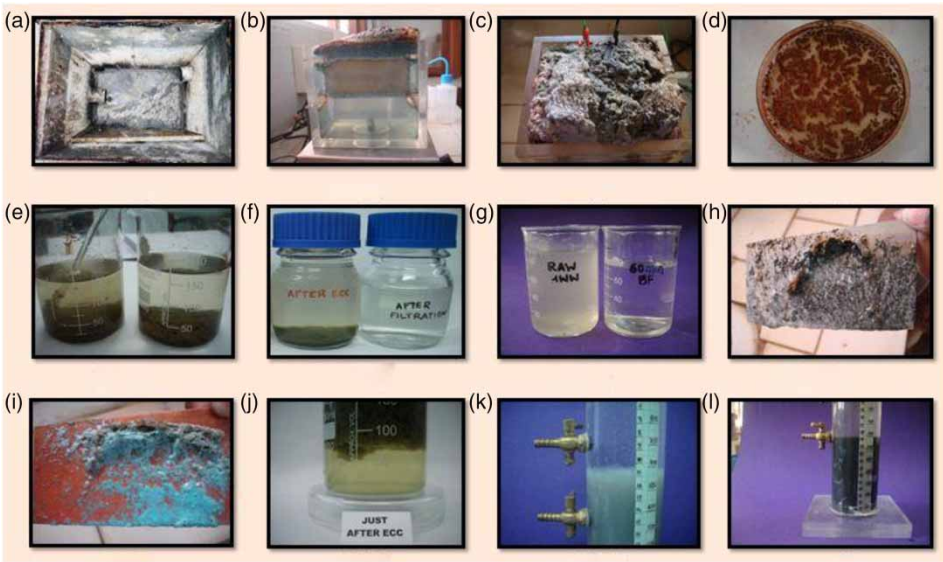

Figure 1 | Various stages during ECC experiments.

were determined using titrimetric analysis. In this work, the quality parameters of focus were O&G, COD and color. The elemental composition of the Fe-ECC sludge was determined using the electron dispersive X-ray spectroscope (EDX) of JEOL JSM-9100 make.

The X-ray diffraction (PROTO Canada) analysis of the post-ECC sludge was carried out to fetch information for its crystalline/amorphous nature.

COD

The COD values of the raw AHWW were determined using Equation (1)

$$\text{COD},\ mg\ L^{-1} = \frac{(A - B) \times M \times 8\ \times 1000}{\text{mL of sample}} \tag{1}$$

where, A is mL of ferrous ammonium sulfate (FAS) for blank, B is mL of FAS for the diluted wastewater sample and M is the molarity of FAS.

O&G

Partition gravimetric method using petroleum ether was used to gravimetrically determine O&G. O&G is determined by solvent extraction using a separation funnel of required volume. A known sample volume was then acidified with 5 mL of HCl. The sample was then transferred to a separator funnel and shaken for 2 min. The solvent is separated from water and evaporated and the residue remaining is used as a measure of the O&G content. After the separation of layers, water is drained off and the solvent containing FOG was transferred to a pre-weighed Petri dish. The solvent was then evaporated in a temperature-controlled water bath. After evaporation, the Petri dish was again weighed and the O&G content was estimated using Equation (2).

$$\text{O\&G},\ mg\ L^{-1} = \frac{(W_2 - W_1) \times 1000}{0.1} \tag{2}$$

where, W_2 is the total weight gain of the tared flask in mg, and W_1 is the calculated residue from solvent blank of the same volume as used in the test.

Color

The total color value of raw AHWW and AH-TRWW samples were estimated using visual comparison method. 1.246 g of potassium chloroplatinate, K_2PtCl_6 (equivalent to 500 mg metallic Pt) and 1.0 g crystallized cobaltous chloride, $COCl_2$, $6H_2O$ (equivalent to about 250 mg metallic Co) was dissolved in distilled water with 100 mL concentrated HCl and diluted to 1,000 mL. This stock solution (standard) has a total color value of 500 PCU (platinum cobalt units). Using the stock solution, subsequent standards having color units of 5, 10, 15, 20, 25, 30, 35, 40, 45, 50, 60 and 70 were prepared by diluting 0.5, 1.0, 1.5, 2.0, 2.5, 3.0, 3.5, 4.0, 4.5, 5.0, 6.0 and 7.0 mL with distilled water.

$$\text{Color units} = \frac{A \times 50}{B} \tag{3}$$

where, A is the estimated color of the diluted sample, and B is mL of wastewater sample taken for dilution.

Chemicals and glassware

Chemicals and reagents were prepared as per standard procedures (APHA 2017). The various chemicals used were standard buffer solution, hydrazine sulfate, hexa methylene tetra-amine, potassium chloride, phosphate buffer solution, magnesium sulfate ($MgSO_4$) solution, calcium chloride, ferric chloride, potassium dichromate ($K_2Cr_2O_7$), sulfuric acid (H_2SO_4), mercuric sulfate ($HgSO_4$), silver sulfate (Ag_2SO_4), standard FAS solution, phenolphthalein indicator, methyl orange indicator, potassium chromate indicator, silver nitrate solution, conditioning reagent, barium chloride crystals, standard sulfate solution, phenol di-sulphonic acid (PDA), potassium hydroxide solution, stock nitrate solution, standard nitrate solution, ammonium molybdate solution, ammonium vanadate solution, potassium chloroplatinate, cobaltous chloride, standard phosphate solution, manganous sulfate, alkali-iodide-azide solution, standard sodium thiosulfate ($Na_2S_2O_3$), sodium chloride (NaCl)

and hydrogen chloride (HCl), and many other chemicals. All the chemicals were of analytical grade purchased from Himedia Laboratories, Mumbai, India. Glassware and instruments used were crucibles, COD vials, COD digester, measuring cylinder, conical flasks, separation funnel, Nessler's tube, settling column (fabricated), filterability column, Buchner funnel, BOD bottles, spectrophotometer, BOD incubator, COD digester, pipette, and desiccator etc. Interferences can occur for determining parameter values when dealing with real wastewaters. A few parameters namely COD, BOD, color, total alkalinity, total solids, sulfate and nitrate were determined by appropriately diluting the raw AHWW to eliminate certain interferences as mentioned in APHA 2017. Raw AHWW and AH-TRWW were not diluted and used as is in ECC batch experiments for removal of target pollutants.

Electrode materials and electrochemical reactor experimental setup

A laboratory-scale cuboid shaped electrochemical reactor (ECR) having a working volume of 1.5 L was fabricated (Figure 1(b)) using see-through organic glass. The cuboidal-shaped ECR offers random movement of colloidal and suspended particles reacting with M^+ ions released in-situ during electrochemical treatment (ECT). Flat plate electrodes of cold-rolled iron of 1.3 mm thick were placed in parallel in the ECR at 1 cm inter electrode distance. Iron electrodes were chosen because of their low cost, high molecular weight and density and commercial availability. The electrodes were cut to rectangular shape (with a triangular projection) of size 10 cm × 5 cm to provide a specific electrode to volume (SA/V) ratio of 40 m^2/m^3 on full submergence of electrodes in the ECR with no moving parts. For supplying current, a DC power supply unit was used. The bipolar electrode arrangement was chosen for easy operations compared to a monopolar arrangement. A monopolar arrangement causes pitting corrosion at active sites of all the anode plates invariably increasing the sludge volume; this condition requires frequent replacement of electrodes, which increase the operating cost of treatment and also cause higher sludge production (Mahesh *et al.* 2006b). Optimal ECC operating process parameters and procedures were established for maximum removal of pollutants and contaminants for both raw AHWW and AH-TRWW with prime focus on achieving short hydraulic retention time (HRT).

RESULTS AND DISCUSSION

Characterization for quality parameters allows proper decision making to choose the kind of treatment suitable for removal of pollutants for the wastewater stream. Therefore, characterization is a pre-requisite for treatment to assess its strength and parameter interlinkage rubrics. Wastewater flow characteristics from ayurvedic hospitals differ significantly from allopathic healthcare wastewater and domestic wastewaters. In addition to high surge volumes during busy hours, the AHWWs typically display high strength compared to domestic wastewaters.

The initial characterization of raw AHWW and AH-TRWW gives values of various quality parameters, which serves as guidelines for choosing the level and degree of treatment, operating conditions and controls. Raw AHWW samples collected from a full-fledged ayurvedic hospital were analyzed for its physico-chemical characteristics. Wastewater samples were also collected from the therapy room (AH-TRWW) and characterized for select parameters listed in Table 1. The pollution control boards in India observes O&G, COD and TDS as prime quality pollution control parameters. Therefore, in this research we focus on these prime quality parameters for removal using electrochemical treatment. Specialized ayurvedic sections in the hospital generate waste streams of medium to high strength, while the combined wastewaters from several activities (housekeeping, food canteen and hospital) generate medium strength as seen by the parameter values in Table 1. It may be observed that O&G, COD and TDS values were high in AH-TRWW compared to AHWW. Lipids is a gross quality parameter representing O&G, fat and long chain fatty acids as organic constituents in the AHWW and AH-TRWW. The distribution and mobility of oxygen, hydrogen, chlorine, ammonia and other gases enhance the flotation of O&G during ECC. The wastewater quality parameter O&G is commonly determined by the methods described in the standard methods (APHA 2017). Also, the total solids content in both the AHWW and AH-TRWW showed high values.

The COD parameter is a more complete and accurate measurement of the total depletion of DO in the receiving waters. High initial COD values in raw AHWW and AH-TRWW show the presence of detergents (surfactants) and sanitizers used for patient treatment activities. COD to BOD ratios >2.8 indicate ineffectiveness of biological treatment methods for achieving adequate mineralization.

Table 1 | Physico-chemical characteristics of raw AHWW and AH-TRWW

No.	Parameters	Discharge standards[a] (inland surface waters)	AHWW	AHWW-TR
1	Flow, Lpd	–	300–600/ bed	100–150/ bed
2	pH	5.5–9.0	7.4–7.9	7.14 ± 0.5
3	Temperature	Shall not exceed 40° C in any section of the stream within 15 m downstream from effluent outlet	25 ± 2 °C	60 ± 5 °C
4	Color, PCU a. Raw b. After Skimming	– –	4,000 2,100	8,000 4,500
5	Total alkalinity, mg/L	–	425–445	560–580
6	Chloride, mg/L	–	120–140	90–110
7	O&G, mg/L	10	400–600	1,170–1,800
8	Total solids, mg/L	–	1,150–1,170	1,600–1,900
9	TDS, mg/L	2,100	810–830	950–1,100
10	Suspended solids, mg/L	100	370–380	650–800
11	COD, mg/L	250	480–520	600–680
12	BOD, mg/L	30	130–180	170–230
13	Sulfate, mg/L	–	27–36	22–34
14	Phosphate, mg/L	–	45–48	30–42
15	Cl^-/SO_4^-	–	3.9–4.5	3–4.2

[a]Environmental Protection Rules 1986.

Mechanism of electrochemical reactions

The reaction mechanism in the electrochemical coagulation treatment process is strongly dependent on the chemistry of the aqueous medium and electrical conductivity (Aouni *et al.* 2009) and also chloride and alkalinity. When the power is switched on, in an EC process, the electro-coagulants are released into bulk solution with kinetic energy levels depending on the applied cell voltage and the corresponding current flowing across the electrodes. Simultaneously, gases such as O_2, H_2, Cl^-, NH_3, N_2, Cl_2, CO_2 etc., are released into the solution depending on the prevailing pH. The oxygen released from the electrode face are nano-micro sized bubbles strong enough to buoy up aggregated electro-flocs as scum to the top of the electrochemical reactor. H_2 and O_2 together can form hydrogen peroxide (H_2O_2) at the approximate manifest pH of the bulk solution (Equation (18)). Further, the oxygen released ultimately reduces the BOD and COD of the treated ECC effluent and has a positive influence on the COD/BOD ratio. Similarly, the chloride content in the wastewater is converted into chlorine gas. Both chlorine gas and H_2O_2 serve as in-situ disinfectants, lysing the pathogenic microbial mass. The general reactions and water quality-related reactions are described through Equations (4)–(11) for iron electrodes.

$$Fe \rightarrow Fe^{2+} + 2e^- \tag{4}$$

$$Fe^{2+} \rightarrow Fe^{3+} + e^- \tag{5}$$

$$Fe \rightarrow Fe^{3+} + 3e^- \tag{6}$$

The divalent and trivalent metal ions follow the Pourbaix pattern and combine with the negatively charged hydroxyl (OH^-) ions and colloids to form the respective hydroxides in the ECR. While using Fe electrodes, the pH value usually increases crossing pH 7.0 reaching a manifest state for a known ET to achieve the desired degree of pollutant destruction. The electrolytic oxidation of iron produces Fe^{2+} ions, which hydrolyze to produce insoluble precipitate $Fe(OH)_2$ and $Fe(OH)_3$ as shown

in Equations (7) and (8).

$$Fe^{2+} + 2OH^- \rightarrow Fe(OH)_2 \quad (7)$$

$$Fe^{3+} + 3OH^- \rightarrow Fe(OH)_{3\ (\text{solid amorphous})} \quad (8)$$

The amorphous solids have a much higher solubility product. The Fe ions liberated into the solution forms iron species following the Equations (9)–(11).

$$3Fe^{3+} + 6OH^- \rightarrow 3Fe\ (OH)_{2\ (\text{green rust})} \downarrow + \frac{1}{2}O_2 \quad (9)$$

$$3Fe(OH)_2 + O_2 \rightarrow Fe(OH)_2 + 2Fe(OOH)_{(\text{yellow brown})} \downarrow + H_2O \quad (10)$$

$$Fe(OH)_2 + 2Fe(OOH) \downarrow + E_2O \rightarrow Fe_3O_{4\ (\text{black})} + H_2O \quad (11)$$

The color of the ECC-treated effluent (Figure 1(b)) and the floating scum (Figure 1(c)) indicate the status of the prevailing electrochemical reactions, showing the kind of hydroxides formed as insoluble precipitates. In addition to dissolution of metal ions, H_2 gas is produced at the cathode and the presence of Cl^- ions in a waste stream result in gaseous Cl_2 bubbles formed at the anode (Hakizimana *et al.* 2017).

Gas formation on the faces of the bipolar electrodes indicate water electrolysis and chlorine oxidation as shown through Equations (12)–(14).

$$2OH \rightarrow \frac{1}{2}O_2 + H_2O + 2e^- \quad (12)$$

$$2Cl^- \rightarrow Cl_2 + 2e^- \quad (13)$$

$$H_2O + 2e^- \rightarrow H_2 + 2OH^- \quad (14)$$

The novelty of the ECC process is that it offers an alkalinity regulation system during treatment. The hydrogen gas released in the formation of metal hydroxide reacts with the alkalinity of the water. The liberated metal ions react with bicarbonate present in the raw wastewater. Dubrawski & Mohseni (2013) showed that alkalinity is generated in-situ in the ECC process following the reactions shown through Equations (15)–(17).

$$Fe^{2+} + 2HCO_3^- \rightarrow Fe(OH)_2 + 2CO_2 \quad (15)$$

$$H^+ + HCO_3^- \rightarrow H_2O + CO_2 \quad (16)$$

$$Fe^{2+} + CO_3^{2-} + H_2O \rightarrow Fe(OH)_2 + 2CO_2 \quad (17)$$

Small quantities of oxygen formed are released and dissolved into the bulk solution. The oxygen dissolved in solution may be reduced to hydrogen peroxide (H_2O_2) as shown in Equation (18). This condition provides disinfection of the treated effluent depending on the solution pH.

$$O_2 + 2H^+ \rightarrow H_2O_2 \quad (18)$$

In this work, during ECC, a black color precipitate (Figure 1(c)) was obtained and after drying, the sludge appeared brick red (Figure 1(d)). This color of the sludge indicates the formation of magnetite (Fe_2O_4) and hematite (Fe_2O_3 and $Fe(OH)_3$) just after drying.

The chlorine gas released into the solution forms chlorine dioxide as shown in Equation (19).

$$Cl_{2(g)} + 4H_2O \rightarrow 2ClO_2 + 8e^- \quad (19)$$

Alkaline ECC treated effluent produce chlorate. In Equation (20), the dissolved ClO_2 takes part in the reactions forming ClO_2^- and ClO_3^- under alkaline conditions of treated AHWW. Chlorate ions undergo electro-reduction to form ClO_2 gas during treatment (Equation 21).

$$2ClO_2 + 2OH^- \rightarrow ClO_3^- + ClO_2^- + H_2O \quad (20)$$

$$ClO_3^- + H_2O + e^- \rightarrow ClO_2 + 2OH^- \quad (21)$$

Chemical complexities may arise from rapid reactions between liberated $Cl_{2(g)}$ gas with ClO_2^- to produce ClO_2 gas (Equation (22)) or with ClO_3^- ions (Equation (23)) depending on the pH of the solution.

$$2ClO_2^- + Cl_2 \rightarrow 2Cl_2 + 2Cl^- \quad (22)$$

$$ClO_2^- + Cl_2 + H_2O \rightarrow ClO_3^- + Cl^- \quad (23)$$

In such operating conditions the salt content measured as chloride (Cl^-) may not reduce in the post-ECC treated effluent.

The nature of electrochemical degradation, though quite complex, follows a logical sequence during treatment. The pollutant removal involves release of M^+ ions, electrochemical oxidation, double layer compression, colloid destabilization, floc formation by physical entrapment, physico-chemico adsorption by electrostatic force of attraction, and finally flotation. The electrochemical degradation process involves the formation of several species of metal hydroxide (Mahesh *et al.* 2006 Part 1), $M(OH)_2^+$, $Fe_2(OH)_2^{4+}$, $Fe(H_2O)_8(OH)_2^{4+}$, as a result of polymerization of hydroxyl species; in addition to the formation of $M(OH)_3$.

Batch ECT studies for optimization of operating parameters

The efficiency of the ECT process, and the cost depends on several operating process parameters and their control limits. The operating parameters are electrolysis time, initial pH, electrode material, current density, electrode spacing and applied cell voltage. The electrode spacing was pre-optimized at 1 cm giving maximum process benefits. An ET of 60 min was identified optimal considering several aspects – current supplied, electrode dissolution, maximum pollutant removal, sludge volume, energy consumption, gravity settling and good filterability. The wastewater quality parameters that grossly influence pollutant removal efficiency are the initial values of total alkalinity, chloride, pH and TDS. External agents/chemical aid/pH adjustment was not necessary, as the favoring quality parameters such as chlorides (total salts) and total alkalinity were adequately available in the raw AHWW before ECC.

Batch electrocoagulation (BECC) of raw AHWW and AH-TRWW was initially carried out using iron (Fe) as sacrificial electrodes. Iron electrodes were chosen as it is easily procurable and to exercise control on producing low SVI values still achieving the desired level of treatment. A good ECC process operation begins by optimizing the cell voltage (or cell current) applied on the electrodes during treatment. Therefore the start-up experiments were carried out for different cell voltages for a pre-optimized ET of 60 min to identify the cell voltage at which maximum pollutant removal occurs. Foam formation was observed during ECT of raw AHWW indicating the presence of surfactants (synthetic detergents). The surfactants lower the surface tension of water and increase its ability to wet surfaces that come in contact with it and emulsifies O&G. Colloid de-flocculation was completely overcome in the ECC treatment process.

Effect of cell voltage on O&G, COD and color removal

Batch discrete ECT experiments were carried out using four Fe plate electrodes applying 2, 4, 6, 8 and 10 V for both raw AHWW and AH-TRWW for 60 min pre-optimized ET. All ECT experiments were carried out in triplicate to obtain consistent pollutant removal, and the average values are reported in the ECC degradation plots.

O&G removal

O&G in wastewaters can cause odor and fly nuisance, slippery surfaces, clog nozzles and filter media, develop slimes and coat walls of settling tanks in wastewater treatment facilities or along the flow pathways. If O&G is not removed from the trade effluent, it interferes with the biological processes presenting issues of oxygen transfer and cause devastating effects on the aquatic food chain. In this work, O&G removal without the need of additional dissolved air flotation (DAF) unit is shown possible using the ECT process. Figure 2 shows O&G removal as a function of cell voltage using an array of 4 iron

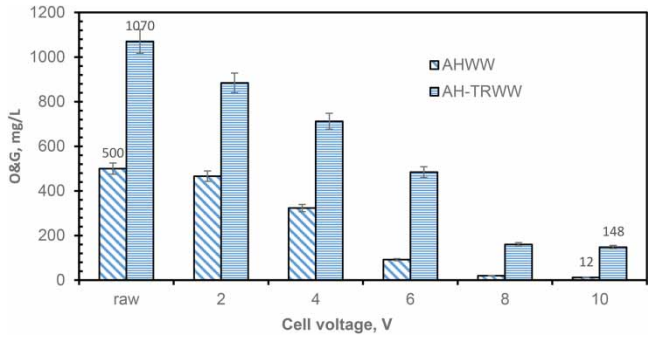

Figure 2 | O&G removal as a function of cell voltage. Operating conditions: 4 Fe electrodes; cell voltage: 2, 4, 6, 8 and 10 V; $O\&G_o$: 500–1,070 mg/L; agitation speed 280–320 RPM; ET: 60 min.

(Fe) plate electrodes for a maximum ET of 60 min for both AHWW and AH-TRWW. For AHWW, O&G removal was 96% with a residual O&G of 20 mg/L at 60 min ET for 8 V, and 12 mg/L for 10 V meeting the PCB discharge norms.

Low O&G removal at cell voltages <6 V is ascribed to the formation of different hydro-complexes. O&G removal is strongly influenced by the cell voltage across the electrodes and the salt content in the wastewater. The in-situ electro-coagulants generated during ECT break-up the oil emulsion into small droplets and simultaneously floc formation in the Pourbaix pH band. The mechanism of O&G removal is by adsorption of destabilized oil micelles on to the electro-flocs with an end effect of flotation by gas bubbles generated during ECT (Rincon & La Motta 2014). An intimate mixture of thousands of micro-bubbles and the floc particles are carried to the surface as froth, and remain atop the electrochemical reactor as scum (as sludge) to be removed later by gravity settling. As a result of sweep flocculation, O&G is removed as destabilized floating scum-gel atop the ECR with high clarity water beneath (Figure 1(b) and 1(g)) for a HRT of <60 min.

COD removal

COD is a measure of the amount of oxidizable matter present in the wastewater indicating the presence of non-bio degradable chemicals and materials. Figure 3 shows COD removal for cell voltages from 2 to 10 V and 60 min ET. Notable changes in COD degradation may be observed for 6 and 8 V onwards for both the wastewaters. The initial chemical oxygen demand (COD_o) for both the wastewaters before ECC ranged from 450 to 640 mg/L. A maximum COD removal of 61 and 64% was achieved for AH-TRWW and AHWW respectively from its initial COD_o of 450 and 640 mg/L for 8 V cell voltage. COD removal for 10 V cell voltage was marginal compared to 8 V. COD being a gross quality parameter; its removal is less compared to O&G ascribed to the following reasons. During ECT, factors such as the salt content (Gotsi *et al.* 2005) in the wastewater, irregular electrode dissolution (Calvo *et al.* 2003) and excess uncontrolled release of iron; add a small quantum of COD to the bulk solution. Hence in this case the net removal of COD is less compared to O&G. All further experiments were carried out for 8 V.

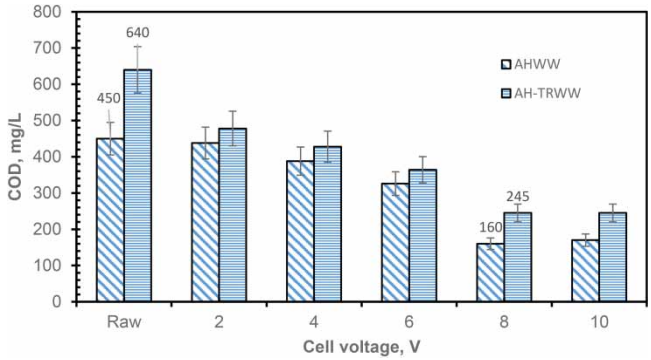

Figure 3 | COD degradation as a function of cell voltage. Operating conditions: 4 Fe electrodes; Cell voltage: 2, 4, 6, 8 and 10 V; COD_o 450–640 mg/L; pH_o 7.14–7.38; agitation speed 280–320 rpm; ET: 60 min.

Color removal

Technically, color of wastewater is either apparent or true. The total color of wastewater is a combination of true and apparent color. The total color units after skimming O&G were 2100 PCU for AHWW and 4500 PCU for AH-TRWW respectively, before ECC. The electrochemical degradation of color for both AHWW and AH-TRWW is shown in Figure 4. For cell voltages <6 V for AH-TRWW, the color of wastewater increases because of dissolution of M^+ ions having less charge into the bulk solution. The M^+ ions so released makes the wastewater dirty and dark increasing the color value at 10–15 min ET on the platinum cobalt scale. For cell voltage >6 V, apparent color removal was consistent leaving the residual true color in the treated effluent. For AHWW, significant apparent color removal was achieved at 8 and 10 V leaving a color residual of 80 PCU in the treated supernatant effluent. The initial raw AHWW was light yellow-brown in color with finely divided solids, and the raw wastewater from the therapy room was light gray in color. After 60 min ET, for >6 V, the ECC-treated effluent was rendered colorless. It was concluded that 8 V of cell voltage was appropriate to achieve maximum apparent color removal at the end of 60 min ET. The true color remaining in the post ECC effluent cannot be removed even at higher applied cell voltages (Golder *et al.* 2005). With excess cell voltage (>10 V) across the electrodes, disproportionate to the amount of pollutants, the possibility of increase in the color value after the appropriate ET is high (Mahesh *et al.* 2006a). The increase in the color value of the treated effluent is because of the increased dissolution of electrode material into bulk solution during ECC (Mahesh *et al.* 2016). The maximum removal of COD, O&G and color from both the wastewaters was achieved applying an optimal cell voltage of 8 V. Ferric ions impart color during ECT (Sahana *et al.* 2018), which are removed later into the floc matrix atop the ECR.

Electrode dissolution

The operating cost depends on the extent of electrode dissolution (ED) for a known cell voltage and ET for a wastewater of known strength. The weight of the electrodes were noted before and after electrolysis for both AHWW and AH-TRWW. Figure 5 shows the total ED of all the four Fe electrodes at the end 60 min ET. In a bipolar arrangement, the anode face

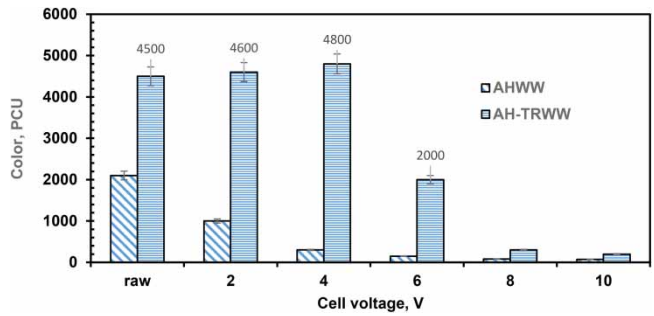

Figure 4 | Color degradation as a function of cell voltage. Operating conditions: 4 Fe electrodes; cell voltage: 2, 4, 6, 8 and 10 V; $Color_o$: 2,100–4,500 PCU; pH_o 7.14–7.38; agitation speed 280–320 rpm; ET: 60 min.

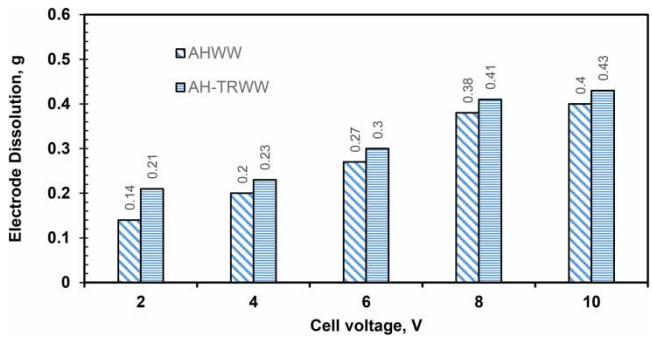

Figure 5 | Electrode dissolution as a function of discrete cell voltage. Operating conditions: 4 Fe electrodes; cell voltage: 2, 4, 6, 8 and 10 V; pHo 7.14–7.38; agitation speed 280–320 rpm; ET 60 min.

of the plate metal dissolves on active spots into the bulk solution releasing M^+ ions. The cathode face of the electrode passivates in the presence of excess $CaCO_3$ (as total hardness) in the wastewater. It was noted that ED increased with increase in cell voltage. The source water used in ayurvedic treatment had low total hardness (TH) values and so passivation was not observed. After maximum pollutant removal at 60 min ET, the ED decreases marginally because of low residual pollutant concentration in the treated effluent (Mahesh *et al.* 2006a); however, the ED continues because of the supplied current. The electro-chemical dissolution of iron electrode is strongly influenced by pH and Cl^- in the raw wastewater. Higher the salt content as Cl^- in the wastewater, higher will be the ED per cubic meter of wastewater treated. Excess current (higher cell voltage) across the electrodes can result in wave corrosion in the presence of high salt content in the wastewater during ECC. This effect can cause increased ED, larger sludge volume, high SVI values, low water reclamation and short life cycle of electrodes, reflecting on the operating cost.

Limiting the cell voltage and the corresponding current is important to exercise control over the above said factors. A cell voltage of 8 V was considered optimal to control the ECC operating system treating AHWW and AH-TRWW. Therefore, all further experiments were carried out for 8 V cell voltage under the set operating conditions for observing post-ECC quality parameter values after ECC at 60 min ET.

O&G, COD and color degradation for optimal cell voltage of 8 V

For an optimal cell voltage of 8 V, prime water quality parameters, removal of O&G, COD and color were intended to be observed during batch ECC degradation experiments in addition to monitoring other pollutants. Initially during ECC, after a lag time the pollutants start to aggregate in the reactor, and at mid ET, flocs begin to agglomerate in the bulk solution. These particles attract and subsequently form large sized flocs with increase in the ET (Nasrullah *et al.* 2020) in the gel-like floc matrix, which float to the top of the ECR. These floc aggregates are able to achieve high vertical settling velocities (v_s) for quick settling by gravity in post-ECC slurry operations. The generation of cationic metal ion concentration increases with ET upto a condition where negatively charged colloids are neutralized and assist in removal of the pollutants/contaminants. The increasing rate of the reaction time is directly proportional to the contaminant removal (Nawarkar & Salkar 2019). As mentioned earlier, four Fe electrodes were arranged in bipolar mode in a 1.5 L ECR. Each ECC experiment was terminated at discrete electrolysis times 15, 30, 45 and 60 min after which the supernatant (excluding scum/sludge) was analyzed for residual O&G, COD, TDS and Cl^-/SO_4^- in the treated effluent followed by settling studies and flux calculations. The ECC process is capable of simultaneous multiple parameter removal, provided the bulk solution characteristics favor the treatment process as described in the following sub-sections.

O&G

O&G parameter analysis requires large sample volumes of 250–1,000 mL raw and treated wastewater. Henceforth, batch experiments were carried out discretely for different ET's to observe the removal pattern of O&G during ECC. The O&G degradation pattern for discrete ET of 15, 30, 45 and 60 min respectively is shown in Figure 6. O&G removal is relatively poor at lower ETs as observed from the plots for AH-TRWW compared to AHWW. A sudden change in slope may be seen in both the degradation curves between 15 and 45 min ET marking the predominance of the second two steps of the

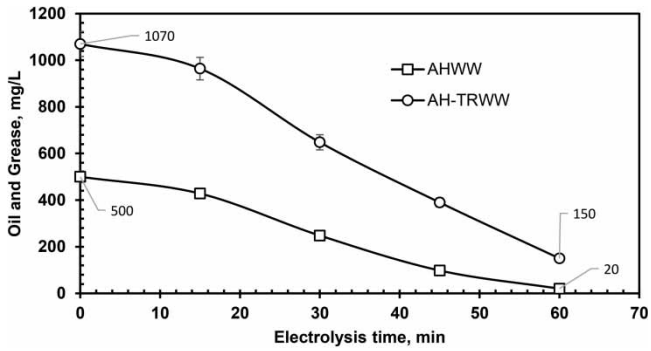

Figure 6 | O&G degradation as a function of discrete ET. Operating conditions: 4 Fe electrodes; cell voltage: 8 V; $O\&G_o$ 450–1,170 mg/L; pH_o 7.14–7.38; agitation speed 280–320 rpm; ET 15, 30, 45 and 60 min.

electrochemical coagulation – flocculation process. At 60 min ET, sweep flocculation manifests removing most O&G from the wastewater giving crystal clear treated effluent, with residual O&G <20 m/L. The positive charge on the released metal ions neutralize the stern and diffuse layers of the negatively charged O&G droplets (Kilany *et al.* 2020). The neutralized matter then coalesces as chain links and bridges by entrapment and buoyed up into the floc matrix. The stirring of the reactor content accelerates the O&G removal process by sweep flocculation. The oil droplets are attracted towards the buoying bubbles, which eventually float to the solution surface and get eventually adsorbed into the ferric hydroxide particles (Yang 2007) in the jelly like scum.

COD

COD removal with ET was observed applying the optimized 8 V cell voltage during ECC as shown in Figure 7. An initial lag time of 10 min was necessary for the solids particles in bulk liquid to adjust to the immediately released M^{+} ions into the solution during ECC for electrical double layer compression. The double layer compression of the negatively charged colloidal particles takes 10 min ET to begin the charge neutralization process as seen in the plots. It may be observed that after 45 min ET, sweep flocculation and enmeshment occurs in a very short time (Figure 1(c)), giving high-clarity treated effluent for AHWW. At the end of the BECT it was observed that COD removal of 54 and 73% was achieved for AH-TRWW and AHWW respectively. The organic compounds present in the real AHWW react with iron ions to form insoluble precipitate (Chou *et al.* 2009). The metal hydroxide species neutralize the electrostatic charges on the dispersed colloidal and suspended particles to reduce the repulsion and enhance floc aggregation (Mollah *et al.* 2001) thus facilitating COD removal.

Color

Figure 8 shows color degradation curves for general AHWW and AH-TRWW up to 60 min ET. The total color value (PCU) increase at 15 min ET and the solution turns a black/gray color (Equation (11)) because of the addition of metal ions resulting in the formation of metal hydroxides Fe_3O_4. The residual 'true color' remaining in solution after 60 min ET was 90PCU and 250PCU for AHWW and AH-TRWW from initial C_o of 2000 PCU and 4600 PCU respectively.

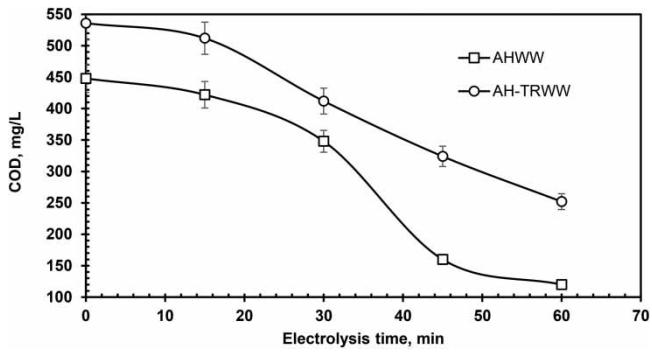

Figure 7 | COD removal as a function of electrolysis time. Operating conditions: 4 Fe electrodes; cell voltage: 8 V; COD_o 450–550 mg/L; pH_o 7.14–7.38; agitation speed 280–320 rpm; ET 15, 30, 45 and 60 min.

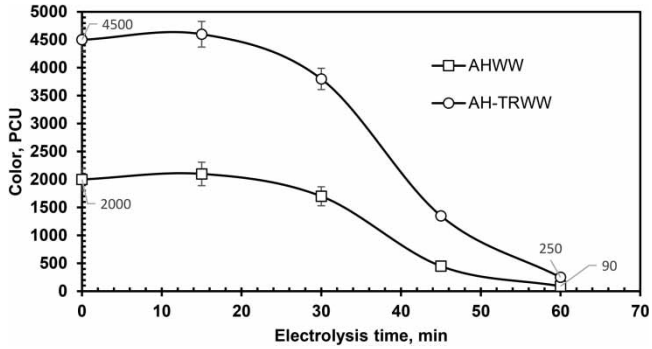

Figure 8 | Color removal as a function of electrolysis time. Operating conditions: 4 Fe electrodes; cell voltage: 8 V; $Color_o$ 2,000–4,500 mg/L; pH_o 7.14–7.38; agitation speed 280–320 rpm; ET 15, 30, 45 and 60 min.

The physical color of the treated effluent appeared dull-gray/black, which disappeared after filtration. The color removal using ECC is controlled (Wang *et al.* 2008) by the production of hydrogen peroxide (Equation (18)) as the oxygen is released from the electrode faces. The residual true color of the treated ECC effluent indicated the presence of dissolved constituents requiring polishing treatment downline the ECC unit. The polishing treatment could be a biological system or an adsorption system known for their ability to remove color causing molecules, dissolved matter and trace metals. After a quiescent time lapse of ~1 h after ECC, the residual true color units of the supernatant increased by 10–15% in the treated effluent indicating the need for immediate filtration just after ECC. At 45 min ET, color removal showed a decrease because iron dissolution continues and the metal oxides do not find any more colloidal particles and suspended particles in the solution (Sajjadi *et al.* 2017). Further, the pH reduction was also noted by a decrease in 1.0–1.5 units with the final pH of the treated effluent within the discharge standards.

TDS

TDS is one of the prime discharge control parameters (EPA 1986). Dissolved solids may be organic or inorganic. Excess accumulation of salts in soil as a result of wastewater discharge tend to increase the soil absorption ratio (SAR). The TDS_o values for raw AHWW and AH-TRWW before ECC were 840 mg/L and 1,060 mg/L. TDS removal for both AHWW and AH-TRWW was 80 and 78% from its initial values. During ECC, the metal ions and the background trace metal ions present in the wastewater increase a little in the first 15 min of ECC. After 15 min ECC, both suspended/colloids and dissolved substances are removed from the solution and reach the scum zone atop the ECR (Figure 1(b) and 1(g)). The marginal removal of TDS after 50 min ET is because of continued metal ions released into the solution and re-entrainment of floating mixed flocs from the scum zone atop the ECR (Figure 9). Higher cell voltages can add dissolved metal ions into the solution increasing the TDS values in the treated ECC supernatant.

ECC of AH-TRWW showed good pollutant removal compared to AHWW because AH-TRWW is a segregated stream containing easily degradable material solids devoid of recalcitrant compounds. The alkaline/acidic sanitizers used as disinfecting agents in housekeeping of different units add up to the inorganic compounds in the AHWW showing relatively lower response to ECC. The heterogenic nature of the combined wastewater from different units refrains it from being electrochemically treated with marginal effectiveness. Apparently, given a higher electrolysis time, the ED tends to increase resulting in a high sludge volume index SVI for the same amount of pollutant removal efficiency. It is then concluded that ECC of segregated/ayurvedic waste stream is more beneficial than treating combined wastewater flow.

Chloride to sulfate (Cl^-/SO_4^-) ratio

Wastewater corrosivity is defined by the ratio of chloride to sulfate concentration measured in mg/L. (Cl^-/SO_4^-) ratio is often considered as one of the corrosion control parameters. Higher this ratio, higher in the corrosion and erosion potential of electrodes. High (Cl^-/SO_4^-) ratios in wastewaters may lead to higher metal dissolution during ECC for a known cell voltage because of higher salt content. Figure 10 shows changes in (Cl^-/SO_4^-) during ECC for 8 V of applied cell voltage for both AHWW and AH-TRWW. Because of the inherent complexity in the electrochemical reactions and random mobility of ions in the solution, variations in the ratio was observed with ET as seen in the plots. The Ca and Mg salts present in the wastewater react with alkalinity (bicarbonate ions) in the solution to form $CaCO_3$ and $MgCO_3$ (Kabdasli *et al.* 2012),

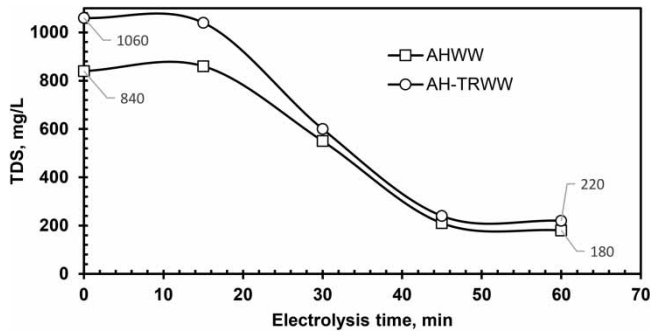

Figure 9 | TDS removal as a function of electrolysis time. Operating conditions: 4 Fe electrodes; cell voltage: 8 V; TDS_o 840–1,060 mg/L; pH_o 7.14–7.38; agitation speed 280–320 rpm; ET 15, 30, 45 and 60 min.

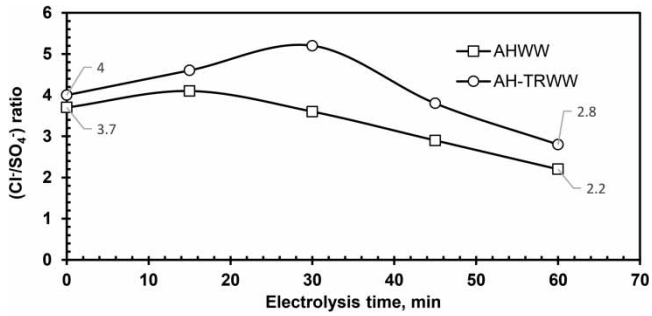

Figure 10 | (Cl^-/SO_4^-) ratio before and after ECC for 60 min ET for AHWW and AH-TRWW. Operating conditions: 4 Fe electrodes; cell voltage: 8 V; (Cl^-/SO_4^-) ratio 3.7–4; pH_o 7.14–7.38; agitation speed 280–320 rpm; ET 15, 30, 45 and 60 min.

which tend to deposit (Equations (24)–(26)) on the cathode faces of the electrode.

$$HCO_3^- + OH^- \rightarrow CO_3^{2-} + H_2O \quad (24)$$

$$CO_3^{2-} + Ca^{2+} \rightarrow CaCO_3 \quad (25)$$

$$CO_3^{2-} + Mg^{2+} \rightarrow MgCO_3 \quad (26)$$

As the relative chloride and sulfate values decrease during ET, the overall (Cl^-/SO_4^-) ratio decreases slightly at the end of 60 min ET marking the utilization of salts during treatment. Using the results obtained on the optimized operating parameters, a check was made to observe the performance of the ECC process using three different electrode materials for the same operating conditions.

ECC performance treating raw AHWW using three different electrode materials, Al, Cu and graphite

Using the cell voltage of 8 V and 60 min ET and 1 cm electrode spacing as optimized operating conditions, the performance of ECC using economically affordable electrode materials like aluminum, copper and graphite (C) were checked for simultaneous removal of O&G, COD, color and TDS for AHWW. The results obtained were then compared with the performance results of iron (Fe) electrodes in batch ECC treatment process.

O&G removal

The presence of O&G in wastewater can foul the treatment system giving an irritating unpleasant odor. Figure 11 shows O&G removal with ET for aluminum, copper and graphite electrodes compared with iron electrodes for 8 V cell voltage for AHWW. It may be seen from the degradation curves that copper electrodes showed less O&G removal during ECC compared to iron electrodes, which showed maximum removal at 60 min ET. When the electrochemical treatment begins, the O&G content in the solution is gradually emulsified, broken into small droplets, and remains suspended for a while in the solution. Iron electrodes could remove maximum (>90%) O&G from the wastewater; while copper showed least removal

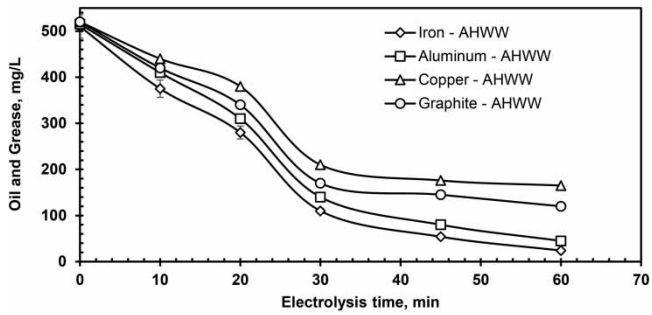

Figure 11 | O&G removal for AHWW as a function of ET for different electrode materials. Operating conditions: 4 Fe, Al, Cu and graphite electrodes; agitation speed 280–320 rpm; ET 10, 20, 30, 45 and 60 min; O&G 480–600 mg/L; cell voltage 8 V.

by ~72% as seen in the plots. Higher O&G removal is surmised to be due to their respective atomic weights and bubble size during ECT. The M^+ ions produced in the reactor during electrolysis destabilizes the suspended oil droplets/particles, attaching with it the gas (CO_2, O_2, H_2, NH_3, Cl_2, HCO_3^-, OCl^- etc.) bubbles and float to the surface of the solution as scum/sludge.

COD removal

COD removal during ECC using four different electrodes was noted as a function of ET for the general raw AHWW. It may be observed in Figure 12, that the COD values decrease with ET leaving soluble COD residues in the bulk solution. A relative comparison between different electrodes materials show that graphite electrodes give lower COD removal (~30%) compared to iron electrodes removing by ~74%. It was noted that, the end pH (pH_f) of the treated effluent at the end of 60 min ET was over 8.0 for all the electrode materials. COD removal was marginal for pH of treated effluent exceeding 9.2 (Kobya *et al.* 2003), indicating high alkaline conditions of the treated wastewater, which do not favor COD removal in the ECC treatment process. It was observed that the solution pH ranging from 7.0 to 7.8 favored pollutant removal while using Fe electrodes. Thin flakes of aggregated floc matter swarmed the anode face of the electrodes (Figure 1(h) and 1(i)) during ECC at the end of the prescribed ET.

Color removal

The initial color value before ECT for raw AHWW was 2050 PCU for raw AHWW**.** In the first 10–15 min, the wastewater in the ECR turns dark and murky adding more color; because of the repulsion effect between moving solids and released M^+ ions. Double layer compression begins after 10–15 min ET followed by the other three sequential steps in the floc manifest process. Solids removed from the system removes apparent color from the raw wastewater being treated. Apparent color removal at 60 min ET was of the order of Fe > Al > graphite > Cu (Figure 13). Fe electrodes delivered crystal clear supernatant after gravity filtration because of the release of polynuclear hydroxyl ions radicals, which react with the negatively charged colloids and neutralize them. The colloidal particles present in the solution are then trapped into these hydroxyl radicals or precipitate, resulting in sweep flocculation, thus removing the apparent color. The removal of residual true color for all electrodes will not be possible because of dissolved and soluble materials that remain after ECT. Unless a few water quality parameters favor the ECC process, there is every possibility that the ECC treated effluent may end up more murky and toxic and non-degradable.

TDS removal

TDS removal was relatively high for Fe and Cu electrodes compared to aluminum and graphite. The TDS remaining in the solution at 60 min ET can increase when most of the suspended and colloidal solids are removed from the bulk solution. It may be noted that the end pH at 60 min ET controls the residual TDS value remaining in the solution (Figure 14). TDS removal for Fe, Al, graphite and Cu electrodes was 64, 56, 59 and 62% respectively (plots not shown). It was noted that poor formation of flocs in the solution during ECC can greatly contribute to the increase in TDS residual values in the ECC-treated effluent, especially at low voltages (Sahana *et al.* 2018).

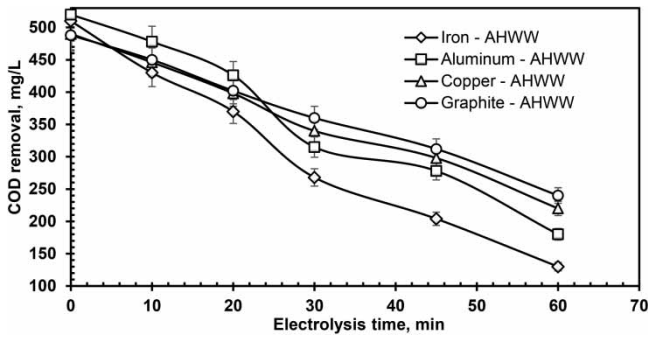

Figure 12 | COD removal for AHWW as a function of ET with different electrode materials. Operating conditions: 4 Fe, Al, Cu and graphite electrodes; Agitation speed 280–320 rpm; ET 10, 20, 30, 45 and 60 min; COD_o 480–520 mg/L; cell voltage 8 V.

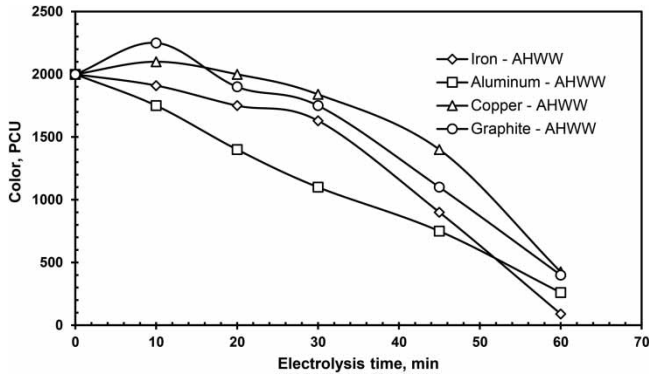

Figure 13 | Color removal as a function of ET with different electrode materials. Operating conditions: 4 Fe, Al, Cu and graphite electrodes; agitation speed 280–320 rpm; ET 10, 20, 30, 45 and 60 min; Color 2000 PCU; cell voltage 8 V.

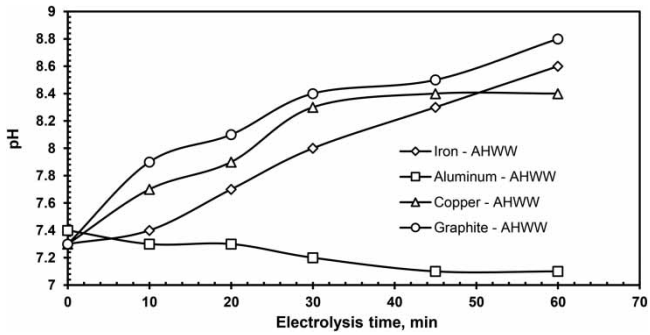

Figure 14 | pH changes as a function of ET with different electrode materials. Operating conditions: 4 Fe, Al, Cu and graphite electrodes; agitation speed 280–320 rpm; ET 10, 20, 30, 45 and 60 min; pH_o 7.13–7.34; cell voltage 8 V.

pH variations during ECT for different electrode materials

Wastewater pH is the key parameter influencing the ECC treatment process and the formation of metal complexes in wastewater (Safari *et al.* 2016). Usually pH increase in the bulk solution is associated with iron, stainless steel and copper electrodes during ECC (Mahesh *et al.* 2006a) except aluminum. Figure 14 shows the pH changes during ECC for Fe, Al, Cu and graphite electrodes. Floc formation takes place at the appropriate pH manifest following the Pourbaix pattern in the presence of adequate alkalinity, at which time most pollutants are removed. The pH regime must stay in the Pourbaix band for hydroxide species to precipitate out of the solution during ECC. A decline in alkalinity values can reduce the pollutant removal and add more color to the solution. In the ECR, when the pH_o is acidic, the final pH in bulk solution increases and when the pH_o is alkaline, the final pH drops (Chen *et al.* 2000). Aluminum electrodes tend to reduce the pH values making the wastewater more turbid and dirty increasing the total solids content and color in the bulk solution of the ECR.

Electrode dissolution

Controlling ED is an integral part of the ECC unit process. The larger the salt content in the wastewater/water, the higher will be the ED depending on current; as a result, electrode life cycle reduces. Figure 15 shows ED for all the electrode materials depending on its position in the ECR in a bipolar arrangement. The anode faces of the electrodes show higher ED by pitting and wave corrosion during electrolysis. The first electrode in the ECR connected to the positive terminal of the DC power supply unit dissolves more than the other three succeeding electrodes. The electrode connected to the negative terminal dissolves relatively less by 90%. High molecular weight iron shows higher ED in 60 min ET, whereas other three electrodes shows less ED. ED control is necessary observing the salt content in the wastewater using the appropriate/optional cell voltage, as it reflects on the SVI values, settling tank design, electrode replacement cycle; capital cost and operating cost of the ECC process.

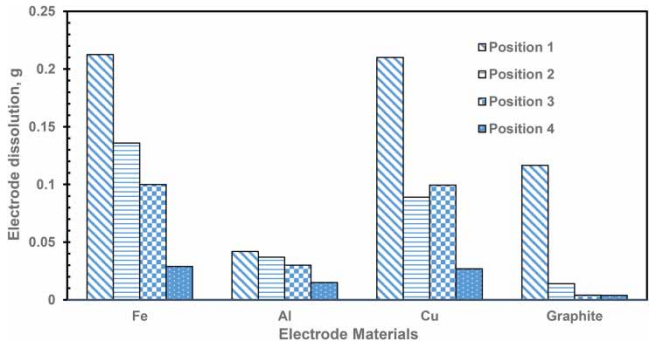

Figure 15 | Electrode dissolution using different electrodes. Operating conditions: 4 Fe, Al, Cu and graphite electrodes; agitation speed 300–320 rpm; ET: 60 min; cell voltage: 8 V.

Sludge-settling characteristics

The quantity of sludge produced during ECC is directly proportional to the applied current, electrolysis time, number of electrodes, anode surface area to volume ratio (ASA/V) total solids content, total alkalinity, and the Cl^- value. To assess the settling potential of ECC slurry gravity settling studies were carried out on the ECC slurry obtained just after treatment using four different electrode materials. Figure 16 shows the sludge-settling pattern for four different electrode materials in the optimized operating conditions. The sludge generated using an aluminum (Al) electrode showed settling resistance because of its low molecular weight, low density and entrapped gas bubbles in the slurry in the first 5 min of the settling process and also because of the polar repulsive forces between the charged electro-floc particles in the discrete settling zone. Iron-generated sludge showed good discrete settling in the first 10 min and compression settling thereafter at 15 min settling time. The discrete particle settling velocity (v_s) in a column entirely depends on the molecular weight of the metal used and bubble size. The higher the molecular weight of the metal, the quicker will be the sludge settling, requiring <25 min to reach the compression zone in the settling tank. A notable observation was that Type II and Type III settling can be entirely eliminated by ECT using the appropriate electrode material and with a pre-optimized set of operating conditions (Mahesh *et al.* 2016). The sludge-settling patterns show the effectiveness of the controlled ECC process inferring that the settling tanks can be designed as compact units with smaller diameters and small side water depth (SWD). With quick settling of solids-floc particles, the settling tank design gives a very small spatial footprint and a compact design. ECC of raw AHWW showed a settling time of <20 min (Figure 1(k) and 1(l)) compared to other high HRT treatment methods that give >40 min settling time. The higher the HRT and settling time, the larger will be the size of the settling tank. The discrete settling velocity of solids particles was 2.67 cm/min for iron slurry and 0.91 cm/min for aluminum electrodes.

SVI

SVI was calculated using Equation (27).

$$SVI = \frac{1000 \times H_{30}}{H_0 \times X_0} \tag{27}$$

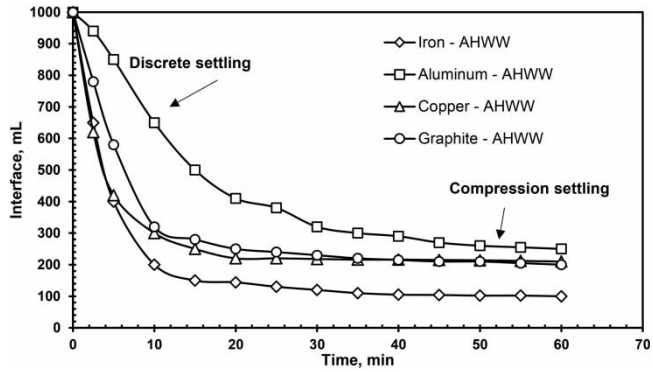

Figure 16 | Sludge interface as a function of time for different electrode materials. Operating conditions: 4 Fe, Al, Cu and graphite electrodes; ET 60 min; pH_o 7.13–7.4; cell voltage: 8 V.

Table 2 | SVI values for different cell voltages for Iron electrodes after 60 min ET for general AHWW and AH-TRWW

	Cell Voltage, V	2	4	6	8	10
SVI	AHWW	No sludge	80	122	148	210
	AH-TRWW	No sludge	110	138	190	390

where H_{30} is the height of the sludge collected at the bottom of the settling column at 30 min settling under quiescent conditions. H_0 is the initial height of the slurry in the settling column, and X_0 is the initial solids concentration of the slurry in mg/L in the entire settling column. Sludge/formation does not occur at low cell voltages (Table 2) because the metal ions released from the active anode face do not have enough positive charge to pick and neutralize negatively charged particles.

As seen from Table 2, the sludge volume increase with the hike in the applied cell voltage. At higher cell voltages the ED is high and therefore higher SVI values are obtained. Lower SVI values show control of sludge production by the cell voltage for the desired pollutant removal, maximizing water reclamation and low residual TDS. Iron electrodes showed lower SVI values (Table 3) compared to the other three electrodes still achieving the desired pollutant/contaminant removal.

Solids flux

The settling velocity (v_s) of ECC generated sludge particles for various initial solids concentration in treated AHWW slurry was conducted repeating several ECC experimental runs at the optimized operating cell voltage of 8 V for 60 min ET. For this purpose, the post-ECC slurry of AHWW and AH-TRWW was either diluted using the treated supernatant or concentrated by removing the supernatant from the settling column. The slurry with different solids concentrations was used to observe the descent of the interface between the sludge and the supernatant in the see-through perspex column. The settling plots showed different settling regimes depending on the solids concentration. For solids concentration >1,136 mg/L, the settling velocity was poor as the solids particles remained in suspension in the column because of minimal interstitial void space between the settling particles. Using the settling data, the variation in sludge settling velocity versus initial solids concentration in the slurry were noted. The sludge settling velocity and the associated flux are important parameters in sizing the settling tank. The solids settling velocity (v_s) and the associated flux is defined as the product of the sludge settling velocity and the solids concentration. The theoretical flux points were determined using the Equation (28).

$$G_i = X_i \times V_i \tag{28}$$

where, G_i is the flux in kg/m^{2}·h, X_i is the solids concentration in kg/m^3 and V_i is the unhindered settling velocity in m/h.

A plot of solids flux as a function of solids concentration for both AHWW and AH-TRWW is shown in Figure 17. The data points at low solids concentration deviate a little for AH-TRWW because of higher solids concentrations in the post-ECC treated effluent and also changing floc particle size during successive repeated settling procedures for the same ECC slurry.

It was noted that the ECC sludge was sturdy and not fragile, which aids in quick settling. The solids flux curve can be employed for sizing the sedimentation tank down line the ECC process.

The EDX analysis of the scum/sludge of AHWW for iron electrodes is shown in Figure 18. The concentration of different common elements is 40.19% C, 48.63% O, 7.92% Fe and other trace elements. The carbon content is twice the value reported of EDX of scum analyzed by Singh *et al.* 2016 treating ayurvedic pharmaceutical wastewater. The higher carbon values in AHWW ECC sludge is because of the presence of more degradable content.

The X-ray diffraction image of the post-ECC sludge is shown in Figure 19, indicating its amorphous nature. However, the presence of crystalline phases of magnetite, iron-hydroxide/oxide, hematite, maghemite and lepidocrocite were identified as by-products as reported by Kim *et al.* 2014 treating wastewater containing heavy metals.

Based on the experimental results, the flow schematic shown in Figure 20 is proposed for treating raw AHWW.

Table 3 | SVI values for different electrode materials at 8 V for general AHWW

Electrode material	Aluminum	Copper	Graphite	Iron
SVI	240	210	205	146

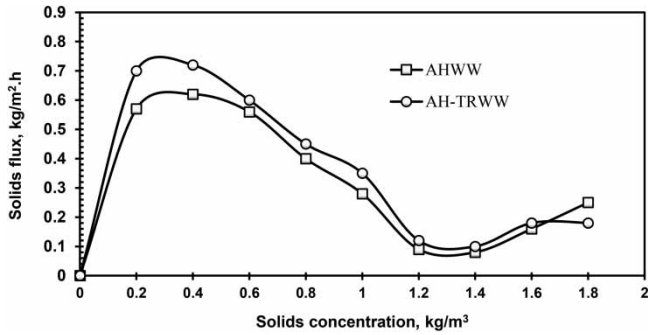

Figure 17 | Solids flux as a function of solids concentration. Operating conditions: 4 Fe electrodes, pHo: 7.13–7.34; cell voltage: 8 V; ET: 60 min; electrode arrangement: bipolar; agitation speed: 280–320 RPM.

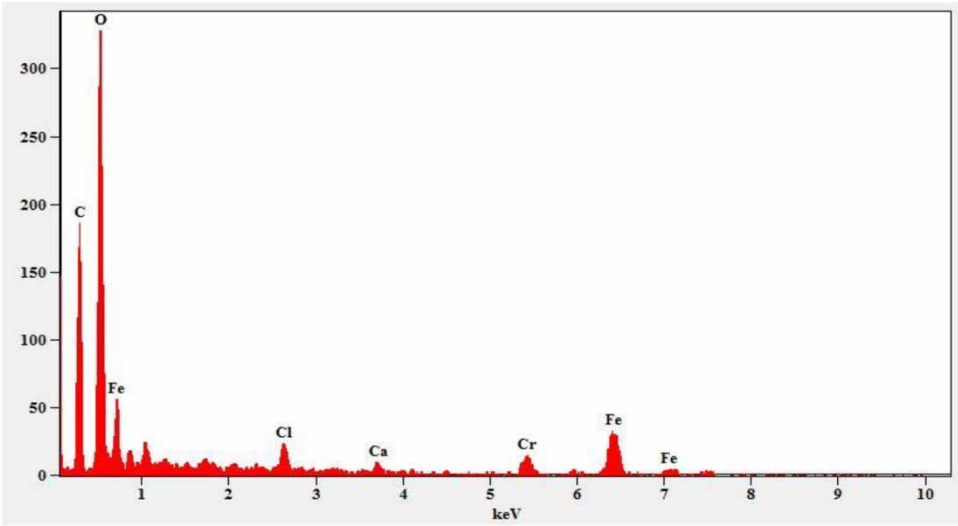

Figure 18 | Elemental composition of Fe-ECC sludge.

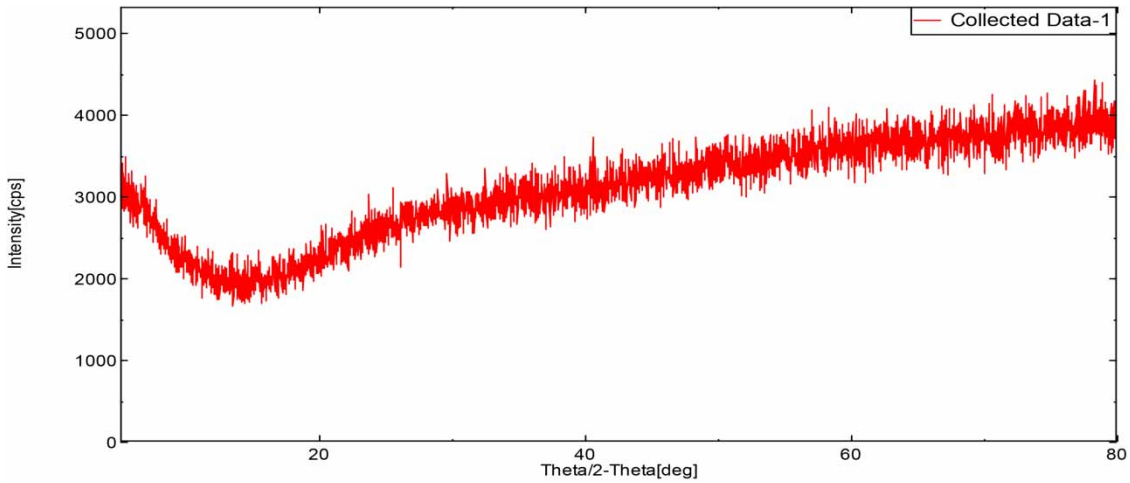

Figure 19 | X-ray diffractogram of AHWW ECC sludge.

Figure 20 | New proposed schematic for treatment of AHWW.

Table 4 | Post-ECC water quality characteristics using Fe electrodes

			Effluent water quality at 60 min ET for 8 V	
No.	**Parameters**	**Raw AHWW characteristics**	**Post ECC**	**After sand filtration**
1	pH	7.4–7.9	8.7	8.5
2	Color, PCU	2,100	90	20
3	COD, mg/L	480–520	130	120
4	O&G, mg/L	400–600	20	5
5	BOD, mg/L	130–180	30	30
6	TDS, mg/L	810–830	180	130

The residual pollutants/contaminants of 18–20% in the ECC treated effluent are believed to have the nature of hydrophobic colloids and dissolved constituents. These constituents do not undergo any kind of further degradation except by way of filtration or adsorption using sand /granular activated carbon, or dual media filtration. The schematic (Figure 20) illustrates that a smaller spatial footprint using ECC is possible compared to the conventional wastewater treatment methods having 8–10 unit operations and unit processes, thus reducing the overall cost of the treatment. Table 4 shows the raw AHWW characteristic values, post-ECC water quality and post-sand filtration water quality. The reclaimed water of 80–82% after simple sand filtration was able to meet the discharge standards of EPA 1986.

CONCLUSIONS

The treatability of AHWW and AH-TRWWW using ECT was investigated using iron electrodes and finding a set of optimized operating conditions. A cell voltage of 8 V and an electrolysis time of 60 min was found optimal for COD, O&G, TDS and color removal; good settlability and filtration, and controlled sludge generation. Iron electrodes showed good removal of color, COD and O&G from raw AHWW compared to Cu, Al and graphite. Iron electrodes also showed low SVI values compared to other electrodes. Solids flux data showed data input for a compact settling tank design and clean water reclamation of 80–82% could be achieved. EDX analysis of AHWW Fe-ECC sludge showed elements containing high levels of carbon (40.19%), oxygen, iron and other trace elements. The XRD pattern displayed an amorphous nature.

The novelty of the ECC process showed its applicability to remove most pollutants/contaminants from raw AHWW giving high-clarity treated water (Figure 1(f) and 1(g)) with water reclamation potential of 80–82%.

ACKNOWLEDGEMENT

The authors acknowledges JSS Mahavidyapeetha, Suttur Srikshetra in Karnataka State for giving an opportunity for pursuing quality Engineering Research under OBE in the Department of Environmental Engineering, Sri Jayachamarajendra College of Engineering, JSS Science and Technology University, JSSTI Campus, Mysuru.

DATA AVAILABILITY STATEMENT

All relevant data are included in the paper or its Supplementary Information.

REFERENCES

Abd El-Gawad, H. S. 2014 Oil and grease removal from industrial wastewater using new utility approach. *Advances in Environmental Chemistry*.

Adhoum, N., Monser, L., Bellakhal, N. & Belgaied, J. E. 2004 Treatment of electroplating wastewater containing Cu^{2+}, Zn^{2+} and Cr(VI) by electrocoagulation. *Journal of Hazardous Materials* **B112**, 207–213.

Aouni, A., Fersi, C., Ali, M. B. S. & Dhahbi, M. 2009 Treatment of textile wastewater by a hybrid electrocoagulation/nanofiltration process. *Journal of Hazardous Materials* **168**, 868–874.

APHA (American Public Health Association) 2017 *Standard Methods for the Examination of Water and Wastewater*, 23rd; (Baird Rodger, B., Eaton Anderw, D., and Rice Eugene, W). American Public Health Association (APHA): Washington, DC, 2017; 1504. 978-0-87553-287-5.

Calvo, L. S., Leclerc, J. P., Tanguy, G., Cames, M. C., Paternotte, G., Valentin, G. & Rostan Lapicque, F. 2003 An electrocoagulation unit for the purification of oil wastes of high COD. *Journal of Environmental Progress* **22**, 57–61.

Chen, G., Chen, X. & Yue, P. L. 2000 Electrocoagulation and electroflotation of restaurant wastewater. *Journal of Environmental Engineering* **126** (9), 858–863.

Chou, W.-L., Wang, C.-T. & Chang, S.-Y. 2009 Study of COD and turbidity removal from real oxide-CMP wastewater by iron electrocoagulation and the evaluation of SEC. *Journal of Hazardous Materials.* **168**, 1200–1207.

Dimoglo, A., Sevim-Elibol, P., Dinc, O., Gokmen, K. & Erdogan, H. 2019 Electrocoagulation/electroflotation as a combined process for the laundry wastewater purification and reuse. *Journal of Water Process Engineering* **31**. https://doi.org/10.1016/j.jwpe.2019.100877.

Dubrawski, K. L. & Mohseni, M. 2013 Standardizing electrocoagulation reactor design: iron electrodes for NOM removal. *Chemosphere* **91** (1), 55–60.

Emmanuel, E., Keck, G., Blanchard, J., Vermande, P. & Perrodin, Y. 2004 Toxicological effects of disinfections using sodium hypochlorite on aquatic organisms and its contribution to AOX formation in hospital wastewater. *Environment International* **30**, 891–900.

Environmental (Protection) Act 1986 *General Standards for Discharge of Environmental Pollutants*. 545–548.

Garcia-Orozco, V. M., Rao-Morales, G., Linarez-Hernandez, I., Serrano-Jimenes, I. J., Salgado-Catarino, A. & Natividad, R. 2021 Electrocoagulation of a chocolate industry wastewater in a downflow column electrochemical reactor. *Journal of Water Process Engineering* **42**, 102057.

Golder, A. K., Hridaya, N., Samanta, A. N. & Ray, S. 2005 Electrocoagulation of methylene blue and eosin yellowish using mild steel electrodes. *Journal of Hazardous Materials* **B127**, 134–140.

Gotsi, M., Kalogerakis, N., Psillakis, E., Samaras, P. & Mantzavinos, D. 2005 Electrochemical oxidation of olive oil mill wastewaters. *Journal of Water Research* **39** (17), 4177–4187.

Hakizimana, J. N., Gourich, B., Chafi, M., Stiriba, Y., Vial, C., Drogui, P. & Naja, J. 2017 Electrocoagulation process in water treatment: a review of electrocoagulation modeling approaches. *Desalination* **404**, 1–21.

Harinarayanan, N. M. G., Manilal, A. M. & Soloman, P. A. 2016 Control of electrocoagulation batch reactor for oil removal from automobile garage wastewater. *Procedia Technology* **24**, 603–610.

He, X., De los Reyes, F., Leming, M. L., Dean, L. O., Lappi, S. E. & Ducoste, J. J. 2013 Mechanisms of fat, oil and grease deposit formation in sewer lines. *Journal of Water Research* **47** (13), 4451–4459.

Kabdasli, I., Arslan-Alaton, I., Olmez-Hanci, T. & Tunay, O. 2012 Electrocoagulation applications for industrial wastewaters: a critical review. *Environmental Technology Reviews* **1**, 2–45.

Keener, K. M., Ducoste, J. J. & Holt, L. M. 2008 Properties influencing fat, oil, and grease deposit formation. *Water Environment Research* **80** (12), 2241–2246.

Kilany, A. Y., Nosier, S. A., Hussein, M., Abdel-Aziz, M. M. & Sedahmed, G. H. 2020 Combined oil demulsification and copper removal from copper plating plant effluent by electrocoagulation in a new cell design. Plating plant effluents by electrocoagulation in a new cell design. *Journal of Separation and Purification Technology.* **248**, 117056.

Kim, D.-G., Palacios Jane, R. S. & Ko, S.-O. 2014 Characterization of sludge generated by electrocoagulation for the removal of heavy metals. *Desalination and Water Treatment* **52**, 909–919.

Kobya, M., Can, O. T. & Bayramoglu, M. 2003 Treatment of textile wastewaters by electrocoagulation using iron and aluminum electrodes. *Journal of Hazardous Materials* **B100**, 163–178.

Kobya, M., Senturk, E. & Bayramoglu, M. 2006 Treatment of poultry slaughterhouse wastewaters by electrocoagulation. *Journal of Hazardous Materials* **B133**, 172–176.

Kumari, A., Maurya, N. S. & Tiwari, B. 2020 Hospital wastewater treatment scenario around the globe. *Current Developments in Biotechnology and Bio engineering*, 549–570. doi: 10.1016/B978-0-12-819722-6.00015-8.

Mahesh, S., Prasad, B., Mall, I. D. & Mishra, I. M. 2006a Electrochemical degradation of pulp and paper mill wastewater part 1. COD and color removal. *Journal of Industrial Engineering Chemistry Research.* **45** (8), 2830–2839.

Mahesh, S., Prasad, B., Mall, I. D. & Mishra, I. M. 2006b Electrochemical degradation of pulp and paper mill wastewater. Part 2. Characterization and analysis of sludge. *Industrial and Engineering Chemistry Research* **45** (16), 5766–5774.

Mahesh, S., Garg, K. K., Srivastava, V. C., Mishra, I. M., Prasad, B. & Mall, I. D. 2016 Continuous electrocoagulation treatment of pulp and paper mill wastewater: operating cost and sludge study. *Journal of the Royal Chemical Society of Chemistry Advances.* **6**, 16223–16233.

Mollah, M. Y. A., Schennach, R., Parga, J. & Cocke, D. L. 2001 Electrocoagulation (EC) – science and applications. *Journal of Hazardous Materials.* **B84**, 2–41.

Nasrullah, M., Singh, L., Krishnan, S., Sakinah, M., Mahapatra, D. M. & Zularisam, A. W. 2020 Electrocoagulation treatment of raw palm oil mill effluent: effect of operating parameters on floc growth and structure. *Journal of Water Process Engineering* **33**. https://doi.org/10.1016/j.jwpe.2019.101114.

Nawarkar, C. J. & Salkar, V. D. 2019 Solar powered electrocoagulation system for municipal wastewater treatment. *Fuel* **2037**, 222–226.

Rajan, R., Robin, D. T. & Vandanarani, M. 2019 Biomedical waste management in ayurveda hospitals current practices and future prospectives. *Journal of Ayurveda and Integrative Medicine* **10**, 214.

Rincon, G. J. & La Motta, E. J. 2014 Simultaneous removal of oil and grease and heavy metals from artificial bilge water using electrocoagulation/flotation. *Journal of Environmental Management* **144**, 42–50.

Sahana, M., Srikantha, H., Mahesh, S. & MahadevaSwamy, M. 2018 Coffee Processing Industrial Wastewater Treatment Using Batch Electrochemical Coagulation with Stainless Steel and Fe Electrodes and Their Combinations, and Recovery and Reuse of Sludge. *Water Sci. Technol. 2018* **78** (2), 279–289. DOI: 10.2166/wst.2018.297.

Safari, S., Aghdam, M. A. & Kariminia, H. R. 2016 Electrocoagulation for COD and diesel removal from oily wastewater. *International Journal of Environmental Science and. Technology* **13**, 231–242.

Sajjadi, S. A., Pakfetrat, A. & Irani, M. 2017 Removal of Remazol Black B dye by electrocoagulation process coupled with bentonite as an aid coagulant and natural adsorbent. *Iranian Journal of Health, Safety and Environment* **5**, 1058–1065.

Sengil, I. A. & Ozacar, M. 2006 Treatment of dairy wastewaters by electrocoagulation using mild steel electrodes. *Journal of Hazardous Materials* **B137**, 1197–1205.

Sharma, S., Aygun, A. & Simsek, H. 2020 Electrochemical treatment of sunflower oil refinery wastewater and optimization of the parameters using response surface methodology. *Chemosphere* **249**. https://doi.org/10.1016/j.chemosphere.2020.126511.

Singh, S., Singh, S., Lien-Lo, S. & Kumar, N. 2016 Electrocemical treatment of ayurvedic pharmaceutical wastewater: optimization and characterization of sludge residue. *Journal of Taiwan Institute of Chemical Engineers* **000**, 1–12.

Wallace, T., Gibbons, D., O' Dwyer, M. & Curran, T. P. 2016 International evolution of fat, oil and grease (FOG) waste management – A review. *Journal of Environmental Management* **187** 1–12.

Wang, C.-T., Hu, J.-L., Chou, W.-L. & Kuo, Y.-M. 2008 Removal of color from real dyeing wastewater by electro-fenton technology using a three-dimensional graphite electrode. *Journal of Hazardous Materials.* **152**, 601–606.

Yang, C. L. 2007 Electrochemical coagulation for oily water demulsification. *Journal of Separation and Purification Technology* **54**, 388–395.

Yasar, A., Dogan, E. C. & Arslan, A. 2013 Macro and micro pollutants and treatment options in hospital wastewaters. *Journal of the Institute of Science and Technology* **2**, 144–158.

First received 25 November 2021; accepted in revised form 22 February 2022. Available online 8 March 2022